Journal of The Electrochemical Society, **153** (12) G1106-G1111 (2006)
0013-4651/2006/153(12)/G1106/6/$20.00 © The Electrochemical Society

Fabrication and Characterization of GaN-Based LEDs Grown on Chemical Wet-Etched Patterned Sapphire Substrates

Y. J. Lee, H. C. Kuo, T. C. Lu, B. J. Su, and S. C. Wang

Department of Photonics and Institute of Electro-Optical Engineering, National Chiao Tung University, Hsinchu 300, Taiwan

Characteristics of GaN-based light-emitting diodes (LEDs) grown on the chemical wet-etched patterned sapphire substrates (CWE-PSS) with different crystallography-etched facets were investigated. An improvement of 40% on the overall quantum efficiency was achieved by adopting this CWE-PSS scheme. A Monte Carlo ray-tracing method was employed to derive the optimized condition of sapphire etching time, and the calculated result demonstrated the same trend with real device measurement. Adopting the CWE-PSS in LEDs could not only improve the epitaxial quality but also increase the extraction quantum efficiency due to crystallography-etched facets efficiently scattering the guided light to enter the escape cone on the top of device surfaces. Finally, we observed better aging behaviors of CWE-PSS LEDs, which could be due to the reduction of threading dislocations of the epitaxial layers.
 [DOI: 10.1149/1.2359701]

Manuscript submitted July 4, 2006; revised manuscript received August 9, 2006. Available electronically October 23, 2006.

III-V nitride wide-bandgap materials have attracted considerable attention in recent years.[1-3] The bandgap energy of AlInGaN varies from 0.8 to 6.2 eV depending on its composition. Therefore, the high-brightness light emitting diodes (LEDs) in these wavelength regions have been widely employed on versatile applications, such as traffic signals, back side lighting in liquid crystal display (LCD), and illumination lighting.[4-6] In general, GaN-based LEDs are grown on the top of the sapphire substrate, and a high dislocation density in the order of 10^8–10^{10} cm^{-2} is induced due to the large mismatch of lattice constant and thermal expansion between the epitaxial GaN film and the underneath sapphire substrate.[7] The large order of magnitude of dislocation density suppresses the further performance of GaN-based LEDs. Additionally, due to the significant difference of the refractive index between the GaN-based material and air, the light extraction efficiency is limited by the total internal reflection. Approximately $1/(4n^2)$ of light from the active region can escape from the top and bottom of the device, where n denotes the refractive index of a semiconductor material.[8] Even though GaN has a lower refractive index ($n \approx 2.5$) than that of other semiconductor materials, only about 4% of the total emitted light can be extracted from one face according to above equation. Therefore, the major effort in fabricating LEDs is then how to get the photons that had been generated inside the active region out of the semiconductor layers. Our group has proposed several methods to enhance light extraction efficiency, including surface roughness and shaping.[9-15] Recently, the single-step growth on the maskless patterned sapphire substrate (PSS) fabricated by dry etching was proposed and a considerable improvement on both internal quantum efficiency and light extraction efficiency was demonstrated.[16-21] Although previous investigations supported the contribution of the PSS fabricated by dry etching, the sapphire surfaces are unavoidably damaged during the dry etching process. Thus, the threading dislocation would easily propagate to the top epitaxial films through GaN layers deposited on the sidewalls of the sapphire patterns whose surfaces have already been damaged, limiting further improvement of epitaxial quality.[22] In this report, we propose a patterned sapphire substrate fabricated by a chemical wet etching technique; hence, the surface damage on the sapphire substrate mentioned above could be eliminated. The details of fabrication and characterization of GaN-based LEDs grown on this novel chemical wet-etched patterned sapphire substrate (CWE-PSS) are discussed and the optimized dimension of the CWE-PSS is also be calculated by the Monte Carlo ray-tracing method.

Device Fabrication

The GaN-based LEDs used in this study were grown using a low-pressure metallorganic chemical vapor deposition (Aixtron 2600G) system onto the C-face (0001) 2 in. diam CWE patterned sapphire substrates. The LED layer structure was comprised of a 30 nm thick GaN nucleation layer, a 2 μm thick undoped GaN layer, a 2 μm thick Si-doped n-type GaN cladding layer, an unintentionally doped active region of 450 nm emitting wavelength with five periods of InGaN/GaN multiple quantum wells (MQWs), and a 0.2 μm thick Mg-doped p-type GaN cladding layer. The as-grown wafer was then patterned with square mesas of 350 × 350 μm^2 size by a standard photolithographic process and was partially etched until the exposure of n-GaN to define the emitting area and the n-electrode a 300 nm thick indium tin oxide (ITO) was deposited as the transparent conductive layer, and Cr/Au was then deposited as n and p electrodes and was alloyed at 200°C in N_2 atmosphere for 5 min. Figure 1 schematically depicts a cross-sectional structure of the GaN-based LED grown on the CWE-PSS. For fabricating the CWE-PSS, the SiO_2 film with hole patterns of 3 μm diam and 3 μm spacing was deposited onto the sapphire substrate by plasma-enhanced chemical vapor deposition (PECVD) to serve as the wet etching mask. The sapphire substrate was then wet etched using an H_3PO_4-based solution at an etching temperature of 300°C. The wet-etching rate for sapphire substrates was about 1 μm/min in this study and can be related to the H_3PO_4 composition and etching temperature.[23,24] Figure 2a and b shows the scanning electron microscopy (SEM) images of the patterned sapphire substrate of the etching time of 90 and 120 s, respectively. In Fig. 2a the crystallography-etched pattern of a (0001)-oriented sapphire substrate has a flat surface of {0001} C-plane with a triangle shape in the center. Surrounding the triangle-shaped C-plane are three facets of {1-102} R-plane with an angle of 57° against the [0001] C-axis. However, due to the relative fast etching rate of C-plane than that of

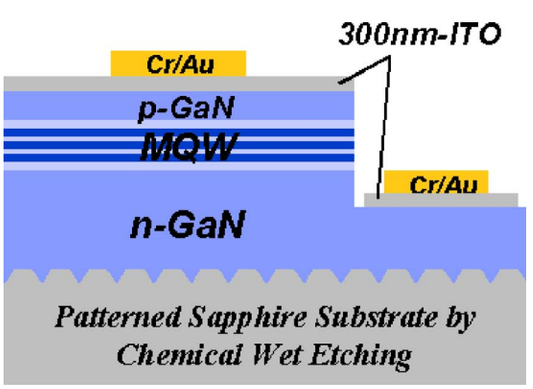

Figure 1. (Color online) The schematic drawing of epitaxial layers and device structure with chemical wet-etched patterned sapphire substrate (CWE-PSS).

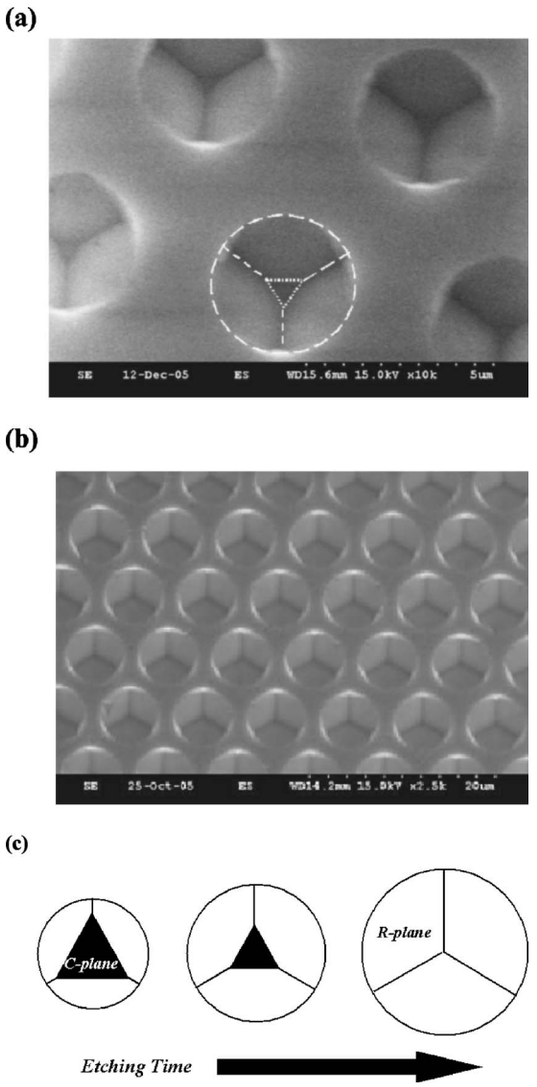

Figure 2. (a, b) SEM images of the CWE-PSS having etching times of 90 and 120 s, respectively. (c) A top-view drawing depicts the evolution of CWE-PSS with the increase of etching time.

R-plane, the triangle-shaped flat surface of the {0001} C-plane in the pattern center finally vanishes with the increase of etching time. As shown in Fig. 2b, the {0001} C-plane disappeared and only the {1-102} R-plane is observed on the CWE-PSS with the etching time of 120 s. Figure 1c shows the evolution of CWE-PSS with the increase of sapphire etching time. The diameter of the sapphire pattern also increases with the increase of etching time due to the side-etching effect; however, the period of the sapphire pattern keeps the same as 6 μm. Additionally, the high slope (57°) crystallography-etched facet of CWE-PSS is hard to fabricate by dry etching, and it has been demonstrated in our previous work that this inclined facet was crucial for improving light extraction efficiency.[15]

To compare the LED performances with different crystallography-etched facet patterns, the sapphire substrates of etching times of 0, 30, 60, 90, and 120 s were employed into this paper. All of these CWE-PSSs were then grown and processed at the same time, eliminating any artificial issue during LED fabrication. The LED chips were packaged into TO-18 without epoxy resin for the subsequent measurement. The typical current–voltage (*I–V*) measurements were performed using a high-current measure unit (Keithley 240). The light output power of the LEDs was measured using an integrated sphere with a calibrated power meter.

Results and Discussion

In order to investigate the film quality of CWE-PSS LEDs, the epitaxial wafers were analyzed by the high-resolution X-ray measurement (Bede D1 HR-XRD). Figure 3 shows the ω-2θ HR X-ray diffraction patterns (XRDs) of the (0002) reflection of the CWE-PSS LEDs. The simulated result of ordinary LED structure was also plotted in this figure for comparison with CWE-PSS LEDs. In Fig. 3, all X-ray measurements of CWE-PSS LEDs were well-fitted with simulated results of ordinary LED structures. Besides, the same location of satellite peaks over the wide measurement range for the conventional (sapphire etching time of 0 s) and all CWE-PSS LEDs indicates that the LED composition and growth rate were not associated with the CWE-PSS.

Figure 4a shows the measurement results of room temperature output power (*L–I* curve) of conventional and CWE-PSS LEDs as a function of the forward-bias current. In this figure, all the CWE-PSS LEDs demonstrate a significant improvement in output power as compared to the conventional LED under our measurement condition up to 200 mA. The enhanced factor of output power of CWE-PSS LEDs compared to the conventional LEDs at a driving current of 20 mA is shown in Fig. 4b. According to this figure, the optimized CWE-PSS condition was achieved at an etching time of 90 s, corresponding to an enhanced factor of 1.4. Figure 4c shows the external quantum efficiency (EQE) of the conventional and CWE-PSS LEDs with the forward injection currents up to 100 mA. It was found that the EQE of the CWE-PSS LED with etching time of 90 s reached a maximum value of about 25% at an injection current of 5 mA and then decreased significantly with a further increase in the forward bias current. Nearly the same trend was also obtained for the conventional LED sample except for a lower EQE value of 17.8%. The degradation at the higher current might be due to overflow of injection carriers and the joule heating effect. Even though the CWE-PSS LED performance in absolute terms of external quantum efficiency does not exceed state-of-the-art devices using other approaches, comparison is being made on the overall intensity enhancement using the CWE-PSS scheme.

In order to study the fundamentals of enhancement of light output with different etching times of CWE-PSS LEDs, we used a commercial ray-tracing software, Tracepro, employing the Monte Carlo algorithm for forward ray-tracing, various outputs including efficiency value, and spatial distributions of radiometric and photometric data. Shape and size of the solid model for the ray-tracing calculation was determined and was exactly the same as the SEM images and microscopic measurements of the geometry of CWE-PSS LEDs, as shown in Fig. 1 and 2. The solid model was built up as a combination of simple solid objects, each semiconductor layer adjacent to the other. According to the recombination process,[25] light rays were generated in the active layer with a uniform random distribution. Monochromatic radiation representing the peak wavelength of the measured spectral emission (450 nm) was used in the simulation. Figure 5 shows the calculated radiation patterns of (a) the conventional and (b) CWE-PSS LEDs with etching time of 30 s. A stronger axial radiation on the CWE-PSS LED than that of the conventional LED was observed in this figure. The same epitaxial models were also built on the other CWE-PSS LEDs with the etching time of sapphire substrate of 60, 90, and 120 s. The comparison of overall light extraction efficiency was plotted and shown in Fig. 5c. According to this calculation, the light extraction efficiency is dramatically enhanced with the increasing of sapphire etching time and over twofold of magnitude of light output was observed on the CWE-PSS LED with the etching time of 120 s. Therefore, the crystallography-etched patterns that evolving with the increasing of etching time of sapphire substrate affect the light extraction efficiency profoundly. With the increase of etching time, the triangle-shaped flat surface of the {0001} C-plane in the pattern center finally vanishes due to its relative fast etching rate than that of the {1-102} R-plane. The sustained {1-102} R-plane has an inclined

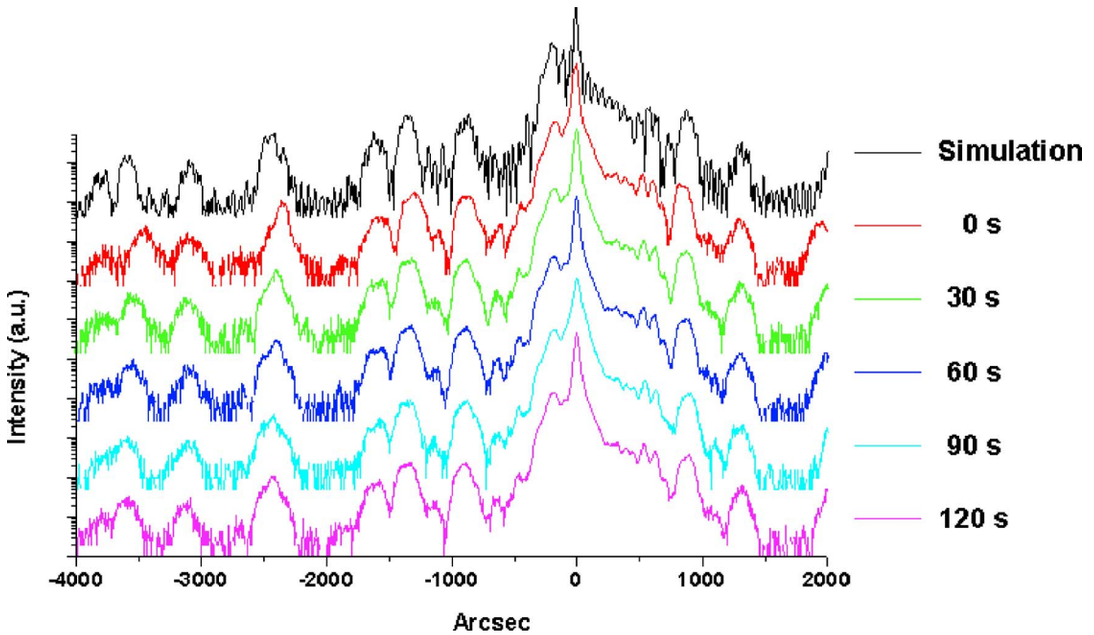

Figure 3. (Color online) High-resolution X-ray measurement (Bede D1 HR-XRD).

crystallography-etched facet with a high slope aslarge as 57°, adding the opportunity of the guided light to meet the escape cone on the top of the chip surface. Figure 6 is a simple schematic ray-tracing of the CWE-PSS LEDs with the increase of sapphire etching time. In the case of the CWE-PSS LED with the large {0001} C-plane pattern, i.e., a short period of sapphire etching time, the light emitting from the LED active region multiple quantum well (MQW) was much easier to be guided inside the LED chip, as compared to that of the longer period of etching time, corresponding to the larger surface of high-slope crystallography-etched facets of {1-102} R-plane. As shown in Fig. 6, more guided light can be extracted from the LED top surface, enhancing the total light output power. This is the reason why in Fig. 5b we can observe strong illumination in the axial direction on the CWE-PSS LED.

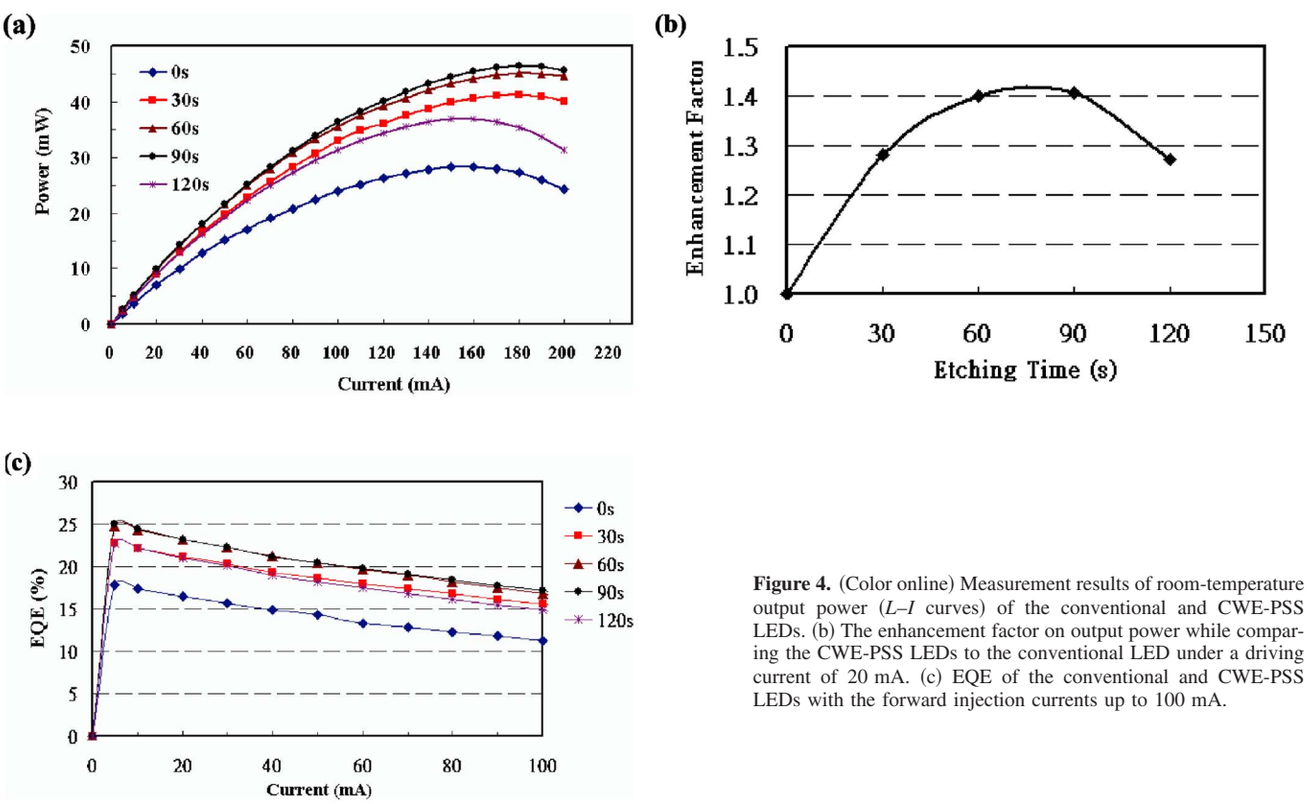

Figure 4. (Color online) Measurement results of room-temperature output power (*L–I* curves) of the conventional and CWE-PSS LEDs. (b) The enhancement factor on output power while comparing the CWE-PSS LEDs to the conventional LED under a driving current of 20 mA. (c) EQE of the conventional and CWE-PSS LEDs with the forward injection currents up to 100 mA.

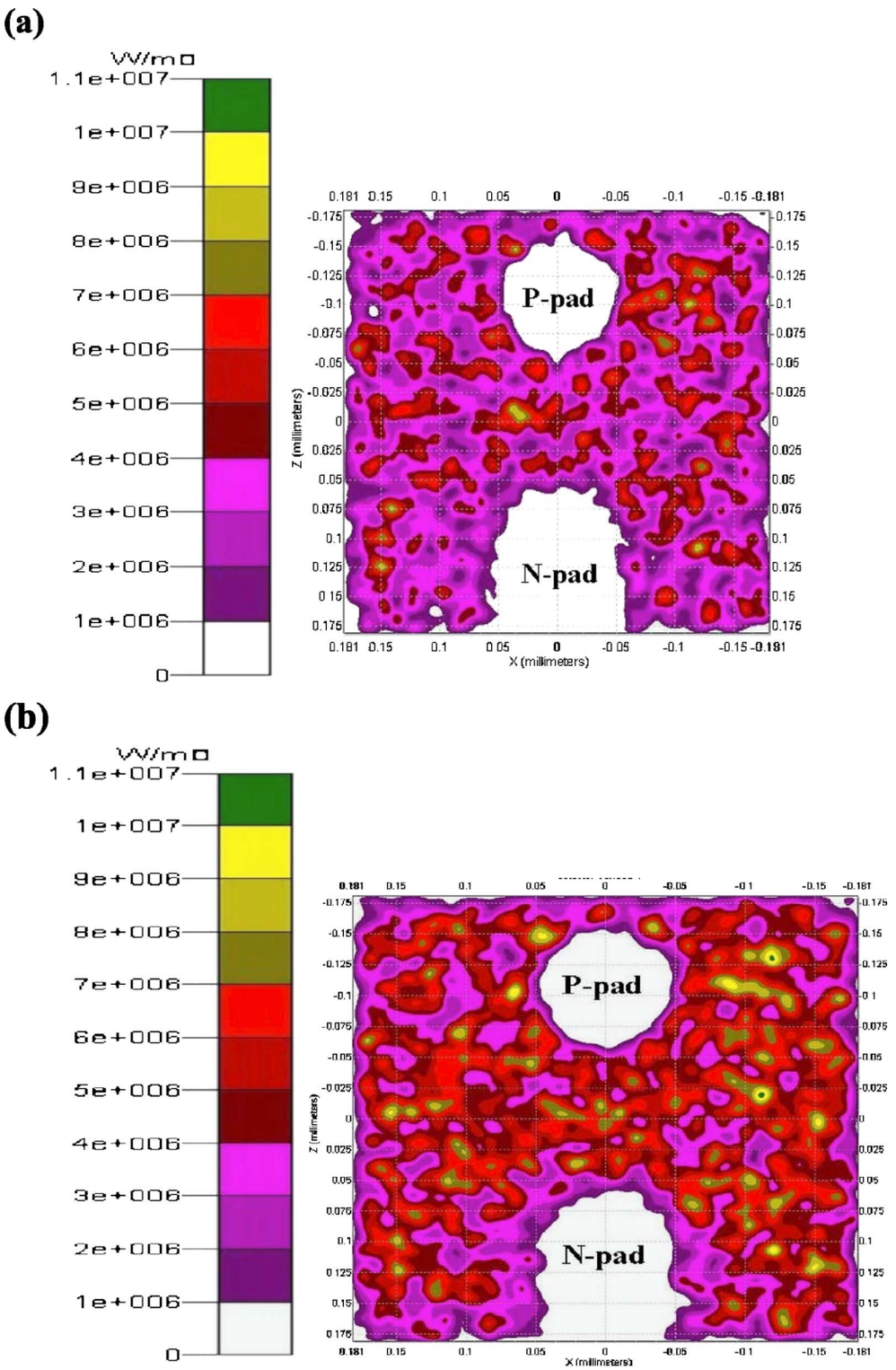

Figure 5. (Color online) Monte Carlo ray-tracing calculated results of radiation patterns of (a) the conventional and (b) CWE-PSS LEDs with etching time of 30 s. (c) Calculated enhancement of the light extraction efficiency with increasing sapphire etching time.

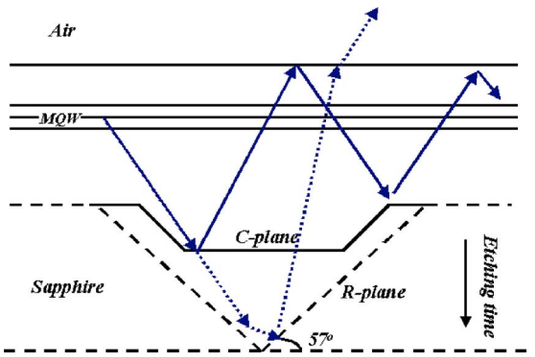

Figure 6. (Color online) A schematic ray-tracing of the CWE-PSS LEDs with increasing sapphire etching time.

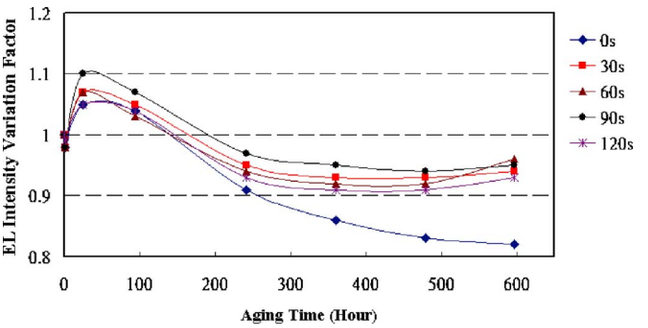

Figure 8. (Color online) Reliability test of the conventional and CWE-PSS LEDs under stress conditions of 55°C and 50 mA.

In comparing the ray-tracing calculation and real device measurement, enhancement of LEDs with etching time of 120 s was degraded probably due to the nonoptimized metallorganic chemical vapor deposited (MOCVD) growth condition. Cross-sectional side-views of SEM images of CWE-PSS LEDs with different etching times are shown in Fig. 7. The crystallography-etched sapphire patterns can be buried completely by the GaN epitaxy in all CWE-PSS LEDs, except for the sample of the etching time of 120 s. According to the ray-tracing calculation, the light extraction efficiency was significantly improved with the increasing of sapphire etching time and could be contributed to the high-slope crystallography-etched facet of the {1-102} R-plane. However, the large inclined crystallography-etched surface also indicates the deep depth of the sapphire pattern, and it also takes more effort for adjusting the growth condition to obtain a high-quality GaN film. As shown in Fig. 7d, a void locating inside the sapphire pattern can be observed due to the relative difficulty for MOCVD to grow on this deep and inclined crystallography-etched facet. Therefore, in the Fig. 4b, a drop of light extraction efficiency was observed on the CWE-PSS LED of sapphire etching time of 120 s. In addition, we did not consider the surface morphology while building the ray-tracing calculation model, where surfaces of LED chips were assumed as perfectly flat. However, as can be seen in Fig. 7, surfaces of LED chips were quite rough; the contribution to output power by adopting the CWE-PSS scheme would be somehow eliminated as compared to the actual device performance in Fig. 4b to the calculation result in Fig. 5c. Nevertheless, by ignoring these epitaxial issues as mentioned above, both the ray-tracing calculation and real device measurement depict the same trend on the enhancement of light extraction efficiency, indicating that the modeling of the LED chip by ray-tracing calculation can be a powerful tool in predicting the efficiency of LED optics designs.

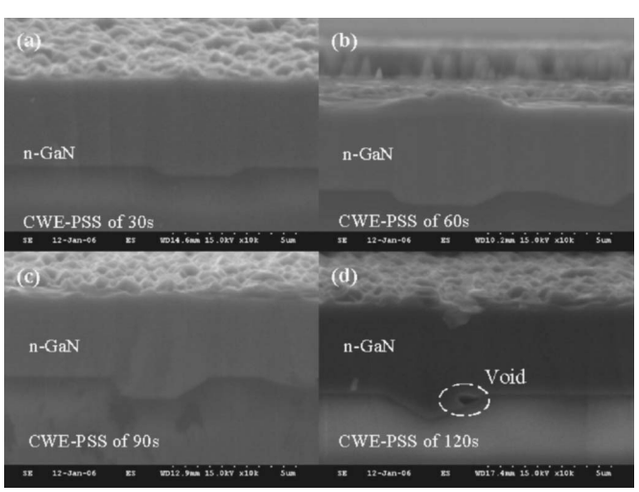

Figure 7. Cross-sectional side-view SEM images of CWE-PSS LEDs with different etching times of (a) 30, (b) 60, (c) 90, and (d) 120 s.

An aging test was performed on the conventional and CWE-PSS LEDs under a driving current of 50 mA at 55°C. In Fig. 8, the EL intensity to the initial EL intensity is shown as a function of aging time. According to this figure, all the aging samples exhibit the same degradation trend. However, all the CWE-PSS LEDs present a gradual degradation in the EL intensity under our measurement condition up to 600 h. In general, the EL intensity of conventional and CWE-PSS LEDs were decayed by about 20 and 10%, respectively; indicating that improvement on the epitaxial quality could be achieved via growth on the CWE-PSS scheme. The better aging behavior of CWE-PSS LEDs could be due to the reduction of threading dislocations of the epitaxial layers. Typically, by employing a patterned sapphire scheme, the epitaxial mode would be shifted from the initial 3D-dominated mode to 2D mode, enforcing threading dislocations bending toward lateral directions, thus improving overall device performances.[16-22] To further identify whether the CWE-PSS scheme could benefit from reduction of dislocation density or the enhancement of internal quantum efficiency, detailed experiments, such as transmission electron microscope or direct measurement of internal quantum efficiency will be investigated in the future.

Conclusion

In summary, the characteristics of GaN-based LEDs grown on patterned sapphire substrate fabricated by chemical wet etching were specifically analyzed. By chemical wet etching, the sapphire substrate exhibited a particular crystallography-etched facet of the {1-102} R-plane with an inclined slope as large as 57°, facilitating a significant enhancement of light extraction efficiency. A Monte Carlo ray-tracing calculation was employed to further investigate the geometric patterns of this novel CWE-PSS LED, and a similar trend was observed between theoretical calculation and the device measurement. Moreover, an improvement of epitaxial quality was also observed on CWE-PSS LEDs, according to device aging results. Therefore, by using this novel CWE-PSS scheme, an overall enhancement of 40% on the quantum efficiency can be achieved that could contribute not only to the improvement of epitaxial quality, but also to the geometrical shape of the inclined crystallography-etched facets, efficiently scattering the guided light to enter the escape cone.

Acknowledgment

The authors thank Professor K. M. Lau of Hong Kong University of Science and Technology and Dr. T. C. Hsu and Dr. M. H. Hsieh of Epistar for useful discussion. This work was supported by the National Science Council of Republic of China (R.O.C.) in Taiwan

under contract NSC 94-2120-M009-007 and NSC 94-2752-E009-007-PAE and was funded by Epistar Corporation, Hsinchu, Taiwan.

National Chiao Tung University assisted in meeting the publication costs of this article.

References

1. S. Nakamura and G. Fasol, *The Blue Laser Diode*, Springer, New York (1997).
2. S. Nakamura, M. Senoh, N. Iwasa, and S. Nagahama, *Jpn. J. Appl. Phys., Part 2*, **34**, L797 (1995).
3. H. Morkoc, S. Strite, G. B. Gao, M. E. Lin, B. Sverdlov, and M. Burns, *J. Appl. Phys.*, **76**, 1363 (1994).
4. M. Koike, N. Shibata, H. Kato, and Y. Takahashi, *IEEE J. Sel. Top. Quantum Electron.*, **8**, 271 (2002).
5. S. H. Lydecker, K. F. Leadford, and C. A. Ooyen, *Proc. SPIE*, **5187**, 22 (2004).
6. J. Jiao and B. Wang, *Proc. SPIE*, **5187**, 234 (2004).
7. S. D. Lester, F. A. Ponce, M. G. Craford, and D. A. Steigerwald, *Appl. Phys. Lett.*, **66**, 1249 (1995).
8. M. Broditsky and E. Yablonovitch, *Proc. SPIE*, **3002**, 119 (1997).
9. C. C. Kao, H. C. Kuo, H. W. Huang, J. T. Chu, Y. C. Peng, Y. L. Hsieh, C. Y. Luo, and S. C. Wang, *IEEE Photon. Technol. Lett.*, **17**, 19 (2005).
10. H. W. Huang, C. C. Kao, J. T. Chu, H. C. Kuo, S. C. Wang, and C. C. Yu, *IEEE Photon. Technol. Lett.*, **17**, 983 (2005).
11. Y. J. Lee, H. C. Kuo, S. C. Wang, T. C. Hsu, M. H. Hsieh, M. J. Jou, and B. J. Lee, *IEEE Photon. Technol. Lett.*, **17**, 2289 (2005).
12. Y. J. Lee, H. C. Tseng, H. C. Kuo, S. C. Wang, C. W. Chang, T. C. Hsu, Y. L. Yang, M. H. Hsieh, M. J. Jou, and B. J. Lee, *IEEE Photon. Technol. Lett.*, **17**, 2532 (2005).
13. Y. J. Lee, T. C. Lu, H. C. Kuo, S. C. Wang, M. J. Liou, C. W. Chang, T. C. Hsu, M. H. Hsieh, M. J. Jou, and B. J. Lee, *Jpn. J. Appl. Phys., Part 1*, **45**, 643 (2006).
14. Y. J. Lee, T. C. Lu, H. C. Kuo, S. C. Wang, M. J. Liou, C. W. Chang, T. C. Hsu, M. H. Hsieh, M. J. Jou, and B. J. Lee, *Semicond. Sci. Technol.*, **21**, 184 (2006).
15. Y. J. Lee, J. M. Hwang, T. C. Hsu, M. H. Hsieh, M. J. Jou, B. J. Lee, T. C. Lu, H. C. Kuo, and S. C. Wang, *IEEE Photon. Technol. Lett.*, **18**, 742 (2006).
16. K. Tadatomo, H. Okagawa, Y. Ohuchi, T. Tsunekawa, Y. Imada, M. Kato, and T. Taguchi, *Jpn. J. Appl. Phys., Part 2*, **40**, L583 (2001).
17. M. Yamada, T. Mitani, Y. Narukawa, S. Shioji, I. Niki, S. Sonobe, K. Deguchi, M. Sano, and T. Mukai, *Jpn. J. Appl. Phys., Part 2*, **41**, L1431 (2002).
18. D. S. Wuu, W. K. Wang, W. C. Shih, R. H. Horng, C. E. Lee, W. Y. Lin, and J. S. Fang, *IEEE Photon. Technol. Lett.*, **17**, 288 (2005).
19. Z. H. Feng and K. M. Lau, *IEEE Photon. Technol. Lett.*, **17**, 1812 (2005).
20. Y. J. Lee, T. C. Hsu, H. C. Kuo, S. C. Wang, Y. L. Yang, S. N. Yen, Y. T. Chu, Y. J. Shen, M. H. Hsieh, M. J. Jou, and B. J. Lee, *Mater. Sci. Eng., B*, **122**, 184 (2005).
21. Y. J. Lee, J. M. Hwang, T. C. Hsu, M. H. Hsieh, M. J. Jou, B. J. Lee, T. C. Lu, H. C. Kuo, and S. C. Wang, *IEEE Photon. Technol. Lett.*, **18**, 1152 (2006).
22. J. Wang, L. W. Guo, H. Q. Jia, Z. G. Xing, Y. Wang, H. Chen, and J. M. Zhou, *Jpn. J. Appl. Phys., Part 2*, **44**, L982 (2005).
23. S. J. Kim, *Jpn. J. Appl. Phys., Part 1*, **44**, 2921 (2005).
24. S. J. Kim, *IEEE Photon. Technol. Lett.*, **17**, 1617 (2005).
25. B. A. E. Saleh and M. C. Teich, *Fundamental of Photonics*, p. 602, John Wiley, New York (1991).